International Journal of Nanomedicine

Dovepress
open access to scientific and medical research

Open Access Full Text Article

ORIGINAL RESEARCH

A Multifunctional Nanozyme Integrating Antioxidant, Antimicrobial and Pro-Vascularity for Skin Wound Management

Tao Jiang[1,2], Weijian Chen[3], Chao Lu[1,2], Jiyong Yang[3], Ziquan Zeng[1,2], Wenqiang Li[4], Hongsheng Liu[5], Nana Huang[5], Yuhui Chen[6], Wengang Liu[1,2]

[1]Department of Orthopedics, Guangdong Provincial Second Hospital of Traditional Chinese Medicine, Guangzhou, 510095, People's Republic of China; [2]Department of Orthopedics, Guangdong Provincial Engineering Technology Research Institute of Traditional Chinese Medicine, Guangzhou, 510095, People's Republic of China; [3]The Fifth Clinical School of Medicine, Guangzhou University of Chinese Medicine, Guangzhou, 510095, People's Republic of China; [4]Engineering Technology Research Center for Sports Assistive Devices of Guangdong, School of Sport and Health, Guangzhou Sport University, Guangzhou, 510500, People's Republic of China; [5]Guangdong Huayan Biomedical Science and Technology Center, Guangzhou, 511441, People's Republic of China; [6]Department of Traumatic Surgery, Center for Orthopaedic Surgery, Third Affiliated Hospital of Southern Medical University, Guangzhou, 510630, People's Republic of China

Correspondence: Wengang Liu, Department of Orthopedics, Guangdong Provincial Second Hospital of Traditional Chinese Medicine, Hengfu Road 60, Yuexiu District, Guangzhou, Guangdong, People's Republic of China, Email liuwengang74@163.com; Yuhui Chen, Department of Traumatic Surgery, Center for Orthopaedic Surgery, Third Affiliated Hospital of Southern Medical University, Guangzhou, 510630, People's Republic of China, Email ah1990726@163.com

Background: Skin wounds are a prevalent issue that can have severe health consequences if not treated correctly. Nanozymes offer a promising therapeutic approach for the treatment of skin wounds, owing to their advantages in regulating redox homeostasis to reduce oxidative damage and kill bacteria. These properties make them an effective treatment option for skin wounds. However, most of current nanozymes lack the capability to simultaneously address inflammation, oxidative stress, and bacterial infection during the wound healing process. There is still great potential for nanozymes to increase their therapeutic functional diversity and efficacy.

Methods: Herein, copper-doped hollow mesopores cerium oxide (Cu-HMCe) nanozymes with multifunctional of antioxidant, antimicrobial and pro-vascularity is successfully prepared. Cu-HMCe can be efficiently prepared through a simple and rapid solution method and displays sound physiological stability. The biocompatibility, pro-angiogenic, antimicrobial, and antioxidant properties of Cu-HMCe were assessed. Moreover, a full-thickness skin defect infection model was utilized to investigate the wound healing capacity, as well as anti-inflammatory and pro-angiogenic properties of nanozymes in vivo.

Results: Both in vitro and in vivo experiments have substantiated Cu-HMCe's remarkable biocompatibility. Moreover, Cu-HMCe possesses potent antioxidant enzyme-like catalytic activity, effectively clearing DPPH radicals (with a scavenging rate of 80%), hydroxyl radicals, and reactive oxygen species. Additionally, Cu-HMCe exhibits excellent antimicrobial and pro-angiogenic properties, with over 70% inhibition of both *E. coli* and *S. aureus*. These properties collectively promote wound healing, and the wound treated with Cu-HMCe achieved a closure rate of over 90% on the 14th day.

Conclusion: The results indicate that multifunctional Cu-HMCe with antioxidant, antimicrobial, and pro-angiogenic properties was successfully prepared and exhibited remarkable efficacy in promoting wound healing. This nanozymes providing a promising strategy for skin repair.

Keywords: Cu-HMCe nanozyme, antioxidation, antibacterial, vascularization, wound healing

Introduction

Skin wounds, whether they result from accidents, surgical procedures, or chronic medical conditions, pose a significant healthcare challenge worldwide.[1–3] Proper wound healing is a complicated and dynamic process associated with various cellular and metabolic activity that must take place in a coordinated and timely manner.[4,5] Failure to achieve optimal wound healing can lead to chronic wounds, increased susceptibility to infections, and impaired quality of life for affected

Received: 28 November 2023
Accepted: 15 March 2024
Published: 4 April 2024

© 2024 Jiang et al. This work is published and licensed by Dove Medical Press Limited. The full terms of this license are available at https://www.dovepress.com/terms.php and incorporate the Creative Commons Attribution – Non Commercial (unported, v3.0) License (http://creativecommons.org/licenses/by-nc/3.0/). By accessing the work you hereby accept the Terms. Non-commercial uses of the work are permitted without any further permission from Dove Medical Press Limited, provided the work is properly attributed. For permission for commercial use of this work, please see paragraphs 4.2 and 5 of our Terms (https://www.dovepress.com/terms.php).

individuals.[6–8] The wound healing process is a meticulously choreographed sequence of events, comprising three overlapping phases: inflammation, proliferation, and remodeling.[9–11] During these phase, inadequate or impaired wound healing can result from a variety of physical and chemical factors, including underlying medical conditions (such as diabetes or vascular disease), poor blood circulation, excessive oxidative stress, uncontrolled inflammation, and bacterial infections.[12–14]

In acute wounds, inflammation plays a crucial and controlled role in the healing process. However, a prolonged and dysregulated inflammatory microenvironment leads to a sustained release of pro-inflammatory cytokines.[15–17] This, in turn, hinders the normal wound healing process, resulting in the development of chronic wounds. In addition, M1 macrophages, which are abundantly present in chronic wounds, produce large amounts of reactive oxygen species (ROS). Under normal physiological conditions, ROS serve as important signaling molecules that regulate several cellular processes such as inflammation and tissue repair.[18] However, excessive production of reactive oxygen species in the wound results in oxidative stress, which impedes vital processes necessary for wound healing, such as the inhibition of angiogenesis and the dysfunction of endothelial cells.[19,20] Moreover, bacterial infections are also a well-known formidable impediment in process of wound healing.[21–23] Among them, *Staphylococcus aureus* (*S. aureus*) and *Escherichia coli* (*E. coli*) are frequently encountered.[24] These bacterial infections further worsen the unfavorable wound microenvironment, hindering the production of extracellular matrix and making it more difficult to achieve timely and effective wound healing.[25]

In promoting wound healing, it is essential to pay attention to the three factors mentioned above, which play a critical role and should not be overlooked. Nevertheless, conventional treatment is incapable of addressing all of these factors concurrently. In recent times, nanotechnology has permitted the exploration of alternative approaches for innovative wound healing therapies. Wang et al synthesized an erythrocyte template nano-enzyme (ETN), which effectively kills methicillin-resistant Staphylococcus aureus (MRSA) by combining peroxidase (POD)-like catalysis with near-infrared (NIR)-induced photo-thermal effect, thereby promoting wound healing.[26] Huang et al constructed functional molecule-mediated Cu^{2+} co-assembled multifunctional nanozymes (Cu-DCA NZs) to promoted healing of diabetic wounds.[27] While there are several nanozymes available for managing skin wounds, many of them do not possess the complete range of antioxidant, antimicrobial, and pro-angiogenic capabilities.

In recent years, cerium oxide nanoparticles have become a subject of great interest in the field of wound healing due to their excellent antimicrobial, anti-inflammatory, antioxidant and angiogenic properties.[28] It has been shown that these nanoparticles can rapidly switch between two oxidation states, Ce^{3+} and Ce^{4+}, resulting in high redox activity.[29] This redox property plays a crucial role in scavenging free radicals and inhibiting bacterial growth. Hollow mesoporous cerium oxide (HMCe) is a unique material consisting of spherical particles with a hollow structure and many mesoporous structures on the surface. Compared to other cerium oxide nanoparticles and hybrid materials, the hollow mesoporous structure of HMCe makes it easier to create functional composites by combining with other materials, modifying the surface of organic or inorganic molecules, loading molecules, etc. and so on to enhance the synergistic impact. Copper (Cu), abundant and inexpensive in nature, is one of the metal elements in the center of natural enzyme activity. Studies have shown that Cu plays a vital role in wound healing, being involved in various cellular processes throughout the different stages of wound healing.[30,31] However, the concentrated release of Cu^{2+} may lead to excessive localized concentrations, causing toxicity. Controlling the rate and concentration of Cu^{2+} release by immobilizing it on the surface or inside of the nanoparticles is an effective solution to deal with Cu^{2+} toxicity. In this regard, Cu-MOF nanoparticles have been widely used in the study of chronic wound healing.[32] However, Cu-MOF particles are large, unstable, structurally fragile, and lack the ability to regulate the complex microenvironment of diabetic wounds. Constructing physiologically stable Cu^{2+}-loaded nanoparticles to achieve slow release of Cu^{2+} while endowing the nanozymes with more functions may be more conducive to synergistic repair therapy for diabetic wounds. Therefore, the combination of Cu nanoparticles and cerium oxide nanoparticles is a novel approach to develop functional wound healing nanomaterials.

Here, a multifunctional nanozyme that integrates all three features for skin wound management was designed and constructed. Hollow mesoporous cerium oxide (HMCe) nanospheres are initially synthesized by a wet chemical method to serve as carrier material, after which copper (Cu) is in-situ co-deposited on the surface of HMCe using the metal reduction method (Scheme 1). Along with good biocompatibility, Cu-HMCe has demonstrated superoxide antioxidant enzyme-mimetic catalytic activity for scavenging reactive oxygen species (ROS) and facilitating wound healing. Both

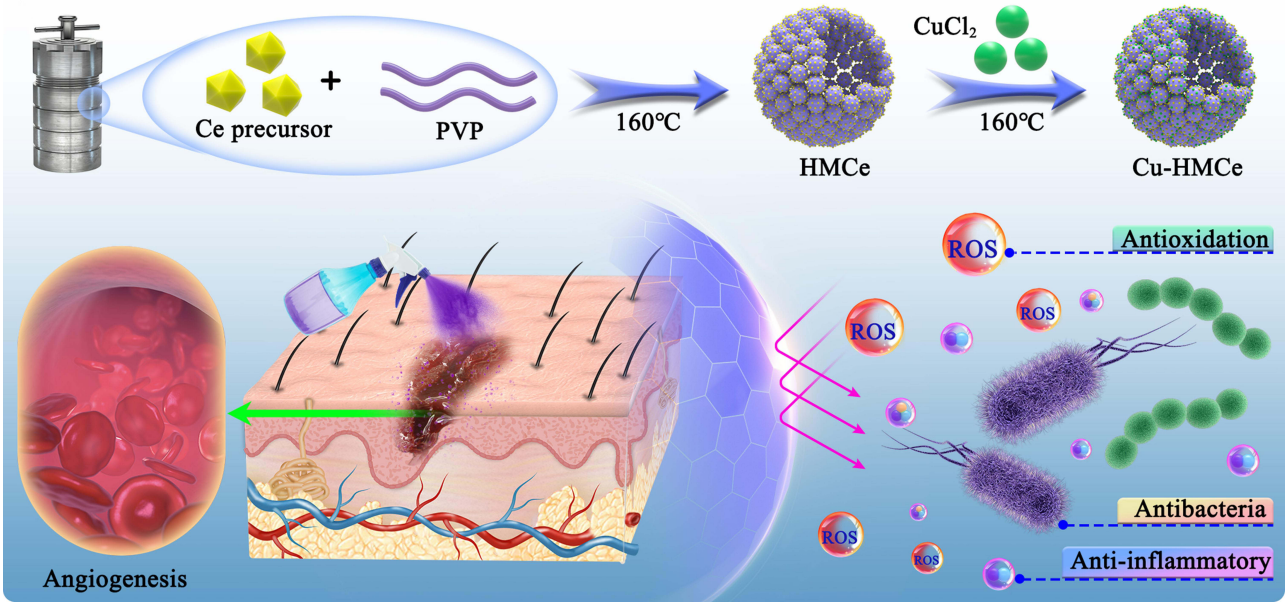

Scheme 1 Schematic illustration showing the copper-doped hollow mesopores cerium oxide nanozyme preparation and its role in the treatment of skin wounds.

in vitro and in vivo studies have provided evidence of the antibacterial properties, anti-inflammatory effects, and angiogenesis-promoting abilities of Cu-HMCe. Thus, Cu-HMCe has the potential to synergistically promote wound healing in several ways.

Experimental and Methods

Materials

Cerium nitrate hexahydrate ($CeN_3O_9{\cdot}6H_2O$, 99.5%, CAS:10125-13-0) were supplied by Aladdin Industrial Corporation (Shanghai, China). Copper (II) Chloride Dihydrate ($CuCl_2{\cdot}2H_2O$, 99.999%, CAS:10125-13-0) was purchased from Sigma Aldrich (Shanghai, China). Tetramethylbenzidine (TMB, 99.5%, CAS:54827-17-7) and 2',7'-Dichlorodihydrofluorescein diacetate (DCFH-DA, CAS: 4091-99-0) were obtained from Beijing Baiaolaibo Technology Co., Ltd (Beijing, China). PVP K30 (CAS:9003-39-8), ethylene glycol (>99%, CAS: 107-21-1), and ethanol (99.7% CAS:64-17-5), were purchased from Shanghai Macklin Biochemical Co., Ltd (Shanghai China). The Cell Counting Kit 8 (CCK-8) was supplied by Nanjng Jiancheng Bioengineering institute (Nanjing, China, CAS:G012).

The Synthesis of Hollow Mesopores Cerium Oxide (HMCe) Nanospheres

Cerium oxide nanospheres were synthesized using a wet chemical method. In brief, an established quantity of cerium nitrate hexahydrate (0.5 g) and PVP K30 (0.2 g) were initially dissolved in 15 mL of ethylene glycol. Subsequently, 1 mL of an aqueous solution containing 1 M HCl was incorporated with vigorous stirring. Following a stirring duration of 30 minutes, the clear solution was moved into a 20 mL autoclave that had a teflon lining. The autoclave was then exposed to a temperature of 160 °C for a period of 3 hours. Upon reaching room temperature, the resultant product, exhibiting a grayish color, was collected and subjected to multiple washes with deionized water for 20 minutes at a speed of 10,000 rpm. For further characterization, the product was then dried overnight at 60 °C. The nanozymes were dispersed in distilled water for particle size and surface charge measurements conducted using an instrument of dynamic light scattering (DLS) (Nano-Brook 90PlusZata, Brookhaven).

The Synthesis of Copper-Droped HMCe (Cu-HMCe) Nanozymes

$CuCl_2{\cdot}2H_2O$ (0.7 mL, 44.8 g/L) aqueous solutions were added to the resulting HMCe products obtained above. The mixture was transferred into an autoclave after stirring for 1 hour, and subsequently, it was subjected to heating at

a temperature of 160 °C for a period of 3 hours in an oven. To obtain Cu-HMCe nanozymes, the mixture underwent centrifugation, followed by three rounds of ethanol washing, and finally dispersed in ultrapure water for future utilization. The surface morphology of Cu-HMCe was examined using scanning electron microscopy (SEM, FEI Corporation, Quanta 250 FEG). Cu-HMCe nanoparticles were dispersed in anhydrous ethanol and added dropwise onto the front side of a copper mesh, which was air-dried at room temperature. Subsequently, the microscopic morphology and elemental composition of Cu-HMCe were analyzed using transmission electron microscopy (TEM, JEOL, JEM-2100F). The elemental composition and valence states of materials were characterized using X-ray photoelectron spectroscopy (XPS, Thermo Scientific ESCALAB 250 XI). The nanozymes were dispersed in distilled water for particle size and surface charge measurements conducted using an instrument of dynamic light scattering (DLS) (Nano-Brook 90PlusZata, Brookhaven).

Evaluation of Biocompatibility in vitro

Human umbilical vein endothelial cells (HUVECs, purchased from Shanghai Hongshun Biotechnology Co., LTD) were employed to evaluate the biocompatibility of the nanozymes. We adopted a variety of methods to test the biocompatibility of materials, including the cell counting Kit-8 (CCK-8), Live/Dead co-staining assay as well as an evaluation of the cellular morphology and cytoskeleton structure. Firstly, the effect of different concentrations of Cu-HMCe on cellular activity was investigated. HUVECs were inoculated into 96-well plates at a concentration of around 5000 cells per well in 100 μL of medium. Following a 24-hour incubation, various concentrations of Cu-HMCe (2.5–80.0 μg/mL) were introduced to the cell culture medium. After an additional 24-hour incubation, the CCK-8 solution was included and incubated for another hour. The results of cellular activity were presented as optical density (OD) measured at 450 nm. Afterwards, the cytotoxicity of HUVECs cultured on Cu-HMCe for varying periods was investigated. Similar to the prior process, the proliferation and viability of HUVECs were evaluated via CCK-8 assay as well as the Live/Dead co-staining assay after 1, 3, and 5 days of co-culturing with Cu-HMCe. The optical density (OD) measured at 450 nm was used to present the outcomes of cellular proliferation, and the cells stained with acridine orange and ethidium bromide were observed using inverted microscopy.

Additionally, the morphology and cytoskeleton structure of HUVECs were examined using a Confocal laser scanning microscope (CLSM) after being co-cultured with the resulting nanozymes. Briefly, after culturing for 3 days, the specimens were immobilized in a 4% paraformaldehyde solution and subsequently made permeable by the inclusion of 0.1% Triton X-100. In order to hinder any unspecific attachment, the specimens were then obstructed employing bovine serum albumin (BSA). Afterwards, rhodamine-conjugated phalloidin (Life Technologies) was utilized to visualize the F-actin filaments in the cells, while 4', 6-diamidino-2-phenylindole (DAPI, Life Technologies) was employed for staining the nuclei. All these procedures were conducted under dark conditions to ensure accurate visualization of the samples.

To assess the effect of nanozymes on the integrity of erythrocytes, hemolytic assay was performed by spectrophotometric measurement of hemoglobin release after erythrocyte lysis. The erythrocytes were collected by taking 1.5 mL of fresh mouse blood, adding it to 3 mL of saline, centrifuging at 1000 r/min for 5 min and centrifuging three times. 970 μL of different concentrations of nanozymes were mixed with 30 μL of erythrocytes and the final concentrations of nanozymes were 5, 10, 20 and 40 μg/mL. Physiological saline-treated water and deionized water were used as negative and positive control groups, respectively. The mixture was incubated on a shaker at 37 °C for 1 h and centrifuged at 1000 r/min for 5 min. The absorbance value of the supernatant at 540 nm was determined by a microplate spectrophotometer. The formula for calculating the percentage hemolysis rate is as follows:

$$\text{Hemolysis Ratio}(\%) = \frac{\text{Abs}_{\text{sample}} - \text{Abs}_{\text{negative}}}{\text{Abs}_{\text{positive}} - \text{Abs}_{\text{negative}}} \times 100\,\%$$

In vitro Assessment of Antibacterial Efficacy

To evaluate the antibacterial effectiveness of the nanozymes, *E. coli* and *S. aureus* were employed for the study. The turbidimetry approach was employed for this assessment. The nanozymes derived from the experiment were cultivated in

LB culture medium alongside 100 μL of bacterial suspension with a concentration of 10^6 CFU/mL. Incubation of each sample occurred on a shaker set at 37 °C for varying durations of 6, 12, 24, or 48 hours. Subsequently, collecting the bacterial suspension and performing turbidimetry analysis at a wavelength of 570 nm, utilizing a microplate reader (Biotek Synergy H1). There were three replications of the experiment in parallel.

Evaluation of Antioxidant Activity in vitro

To assess the ability of antioxidant compounds, a range of methods for measuring antioxidant activity have been employed. Firstly, a free radical-eliminating assay was conducted using a classic 2,2-Diphenyl-1-picrylhydrazyl (DPPH) free radical experiment to investigate the antioxidant enzyme-mimetic activities of Cu-HMCe. Subsequently, HUVEC cells were introduced into confocal dishes or 6-well plates, at respective densities of 5.0×10^4 or 2.0×10^5 cells per well, and incubated for a period of 24 hours. After that, PBS, HMCe, or Cu-HMCe were applied to the cells for a duration of 12 hours. To evaluate the results, the treated cells were stained with 10 μM DCFH-DA solution and incubated in a dark environment at a temperature of 37 °C for a duration of 30 minutes. The cells were observed using LSCM or analyzed using flow cytometry after washing three times with PBS. Meanwhile, the ability of Cu-HMCe to scavenge free radicals at different time points was also investigated.

In addition, the resulting nanozymes were subjected to ·OH scavenging ability test using 3.3',5,5'-tetramethylbenzidine (TMB) measurements. The hydroxyl radical (·OH) was produced through the conventional fenton reaction of H_2O_2 and Fe^{2+}. This reaction leads to the conversion of TMB to oxidized TMB (oxTMB), characterized by a distinctive absorbance at 652 nm. Hence, the remaining concentration of ·OH can be measured by monitoring the absorbance of oxTMB at 652 nm. In addition, the electron paramagnetic resonance spectrometer (JES-FA200, JEOL, Ltd., Japan) was utilized to examine the effectiveness of the resulting nanozymes in scavenging hydroxyl radicals (•OH), using DMPO as the scavenger. Briefly, a solution comprising of DMPO (40.0 mM), resulting nanozymes (100.0 $\mu g\cdot mL^{-1}$), and H_2O_2 (10.0 mM) was prepared and analyzed.

Angiogenesis Ability of Nanozymes

To investigate the effect of resulting nanozymes on the pro-angiogenic capacity of HUVECs, cell migration assays along with tube formation assays were performed in vitro. For the cell migration assays, HUVECs were planted in 24-well plates at a cell density of 4×10^4 per well and incubated until they reached approximately 90% confluence. Subsequently, using a 200 μL sterile plastic tip to create a scratched area. The corresponding wells were then treated with the fresh culture medium containing different resulting nanozymes and co-cultured for 24 hours. The relative distance traveled by the wounded cells was measured by an inverted microscope to observe the migration of the cells. For the analysis of angiogenesis, a 96-well plate was prepared by coating it with 10 μL of Matrigel on ice. The plate was incubated at 37 °C for 30 minutes. Subsequently, HUVECs were inoculated into each well at a cell density of 5000 cells per well. Afterward, the cells were treated with either PBS or various resulting nanozymes. The formation of tubes was assessed at 12 and 24 hours using an inverted microscope. Vascular nodes and branches were measured as indicators of tube formation and quantified using Image-J software.

Furthermore, to evaluate the neovascularization capacity of HUVECs, extracellular proteins (CD31) were subjected to immunofluorescence staining. HUVECs were inoculated into confocal dish at a cell density of 2×10^4 cells per well and cultured overnight. Following this, the cells were exposed to various nanozymes or PBS for a duration of 24 hours. The treated cells were washed with PBS and then fixed with a 4.0% solution of paraformaldehyde. After fixation, the cells were incubated with anti-CD31 antibodies for a duration of 24 hours. Subsequently, DAPI staining was performed for 15 minutes and their observation was carried out using CLSM.

In vivo Wound Healing Experiments

In this study, Sprague Dawley (SD) male rats were used to observe the promotional effect of nanozymes on wound healing in vivo. Our animal procedures were conducted in accordance with the Guidelines for the National Research Council's Guide for the Care and Use of Laboratory Animals and were approved by the Animal Ethics Committee of Guangzhou Sport University (Ethical certificate number: 2023DWLL-35). The rats were divided into four groups, including the treating with PBS group (control group), the treating with Cu^{2+} group, the treating with HMCe group,

and the treating with Cu-HMCe group. First, SD rats were anesthetized with pentobarbital sodium (30 mg/kg), and were created a full-thickness 10 mm diameter circular wound in the dorsal region using a 10 mm puncture perforator. After removing the wounded skin, a 10 μL suspension of *E. coli* (1.0×10^6 CFU/mL) was evenly applied to the wound surface and left to dry naturally. This procedure established a model of circular bacterial infection. Subsequently, the wounds were treated with 200 μL of PBS or 200 μL of PBS containing different concentrations of Cu^{2+}, HMCe, and Cu-HMCe solutions, respectively, according to the grouping. The wound size of each sample rat was recorded using a digital camera every day for 14 days after surgery, and the wound closure area was estimated using Image J software. On days 3, 10, and 14, rats were euthanized, and skin tissue from the wounds were collected and preserved in 4% paraformaldehyde tissue fixative. The collected skin tissue sections were subjected to H&E staining, Masson staining and immunohistochemical analysis. Firstly, the slices were fixed, washed and embedded in paraffin, and sliced at 5 μm. The sections collected on the 14th day were then stained with H&E and Masson trichrome, and the sections taken on the 3rd and 10th day were stained with immunofluorescence antibodies for tumor necrosis factor-α (TNF-α), interleukin-6 (IL-6), and Platelet endothelial cell adhesion molecule-31 (CD31). Staining steps were performed according to standard protocols. Microscopy was used to observe and photograph the slides. The wounds were evaluated histologically at each time point in each group and the images presented were representative of all replicates.

The neovascularization ability was evaluated by assessing the positive α-SMA and CD31 immunofluorescence in the tissue sections. Firstly, tissue slides coated with paraffin were subjected to an overnight incubation at 4 °C with immunofluorescence antibodies against CD31 or α-SMA, and then the slides were incubated with rhodamine-conjugated goat anti-rabbit or fluorescein isothiocyanate (FITC) -conjugated goat anti-mouse secondary antibody for 30 minutes. For visualization, the nuclei were stained with DAPI. The results were observed by CLSM.

Statistical Analysis

The experimental data are expressed as mean ± standard deviation (SD). All experiments were repeated at least three times, and statistical analysis was carried out using GraphPad Prism software with ANOVA/Tukey's test or Student's *t*-test. Significance levels of $*p< 0.05$, $**p< 0.01$, and $***p<0.001$ were applied.

Results

Construction and Characterizations of Nanozymes

The Cu-HMCe nanozyme was synthesized using a simple and rapid method. SEM and TEM images showed that the Cu-HMCe particles exhibited a spherical shape with a size of about 100–200 nm. The nanozyme possessed a mesoporous structure and a slightly rough surface (Figure 1A and B). These unique structures could promote a slow but sustained release of Cu, resulting in the longer-lasting activity of Cu-HMCe. The rough surface morphology of Cu-HMCe may be due to the deposition of copper oxide. Besides, the mapping images of energy dispersive spectroscopy showed a consistent dispersion pattern of Cu (purple), Ce (yellow), O (green), and N (red) within the nanozyme (Figure 1C). The presence of Cu, Ce, O, and N elements was further validated through X-ray photoelectron spectroscopy (XPS) analysis (Figure 1D). The high-resolution Cu 2p spectrum of Cu-HMCe exhibited characteristic peaks at approximately 954.3 eV and 934.1 eV, corresponding to Cu 2p1/2 and Cu 2p3/2 states, respectively (Figure 1E). The Cu 2p spectrum and the existence of O 1s peaks in the XPS spectra suggested that the Cu element in Cu-HMCe occured in Cu^+ and Cu^{2+} oxidation states. Similarly, the Ce 3d spectrum of Cu-HMCe revealed a mixture of Ce^{3+} and Ce^{4+} states (Figure 1F). The characteristic peaks at approximately 724.78 eV and 710.58 eV were attributed to Ce 3d3/2 and Ce 3d5/2 states, respectively.

To demonstrate the impeccable assembly of Cu-HMCe, we also conducted dynamic light scattering (DLS). The results revealed that the hydrodynamic size of Cu-HMCe in distilled water was 143.4 ± 4.3 nm, significantly larger than that of HMCe (~ 135.1 ± 3.3 nm, as shown in Figure 1G and H), indicating the deposition of CuO on the surface of HMCe. Additionally, the surface of cerium oxide nanoparticles is negatively charged due to carrying a large number of carboxyl groups. The zeta potential of Cu-HMCe was higher than that of HMCe, which was attributed to the shielding effect of CuO deposition on surface charges (Figure 1I). Taken together, the above results provided confirmation of the successful preparation of Cu-HMCe.

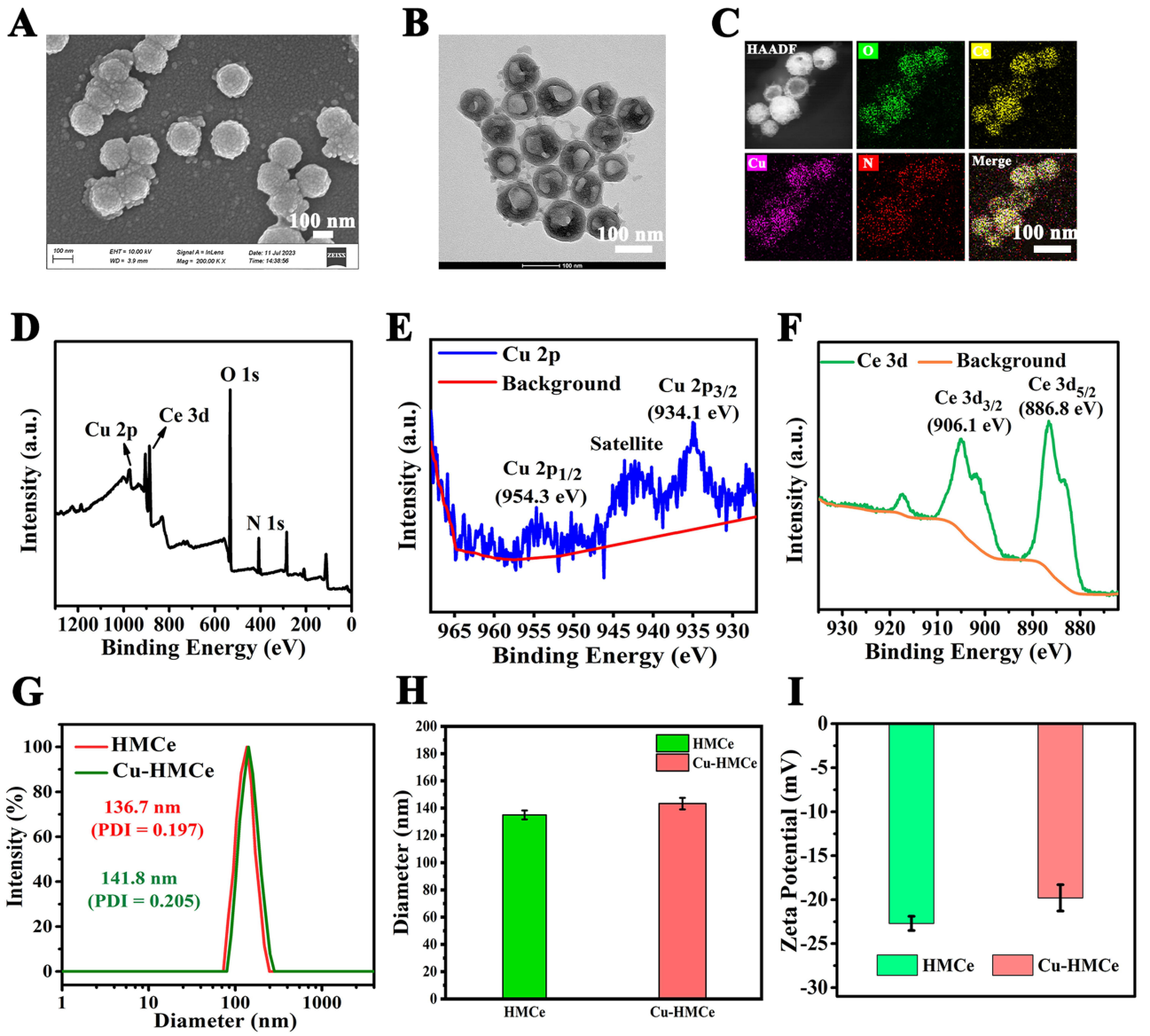

Figure 1 Characterization of Cu-HMCe. (**A**) The SEM image and (**B**) TEM image of Cu-HMCe. (**C**) SEM images of Cu-HMCe and energy dispersive X-ray mapping of Cu, Ce, Cu and N elements. (**D**) XPS spectra of Cu-HMCe. The high-resolution spectrum of (**E**) Cu 2p and (**F**) Ce 3d. (**G**) The particle size distribution, (**H**) hydrodynamic size and (**I**) zeta potential of the Cu-HMCe.

Biocompatibility Evaluation of Nanozymes

Favorable biocompatibility is an important indicator for nanozymes. Therefore, we adopted a variety of tests to investigate the biocompatibility of Cu-HMCe. The results of CCK-8 demonstrated that HUVECs maintained a cell viability of over 80% even when exposed to high concentrations (80 μg/mL) of Cu-HMCe (Figure 2A). Moreover, there was no significant difference in PBS, HMCe, and Cu-HMCe groups after a 5-day treatment (Figure 2B). The Figure 2C displayed the live/dead staining of HUVECs in response to 3 days of culture on control, HMCe, and Cu-HMCe. The results demonstrated that both HMCe and Cu-HMCe were compatible with cell activity. Besides, the cell morphology observations analysis revealed that HUVECs cultivated on Cu-HMCe had a larger spreading area compared to the control and HMCe group. Furthermore, the HUVECs on Cu-HMCe exhibited a distinct elongated spindle-like shape with well-defined pseudopods (Figure 2D). The above results suggest that Cu-HMCe exhibits good cytocompatibility, the addition of Cu did not adversely affect the cells. Whatmore, the appropriate concentration of Cu^{2+} had a positive effect on cell growth.

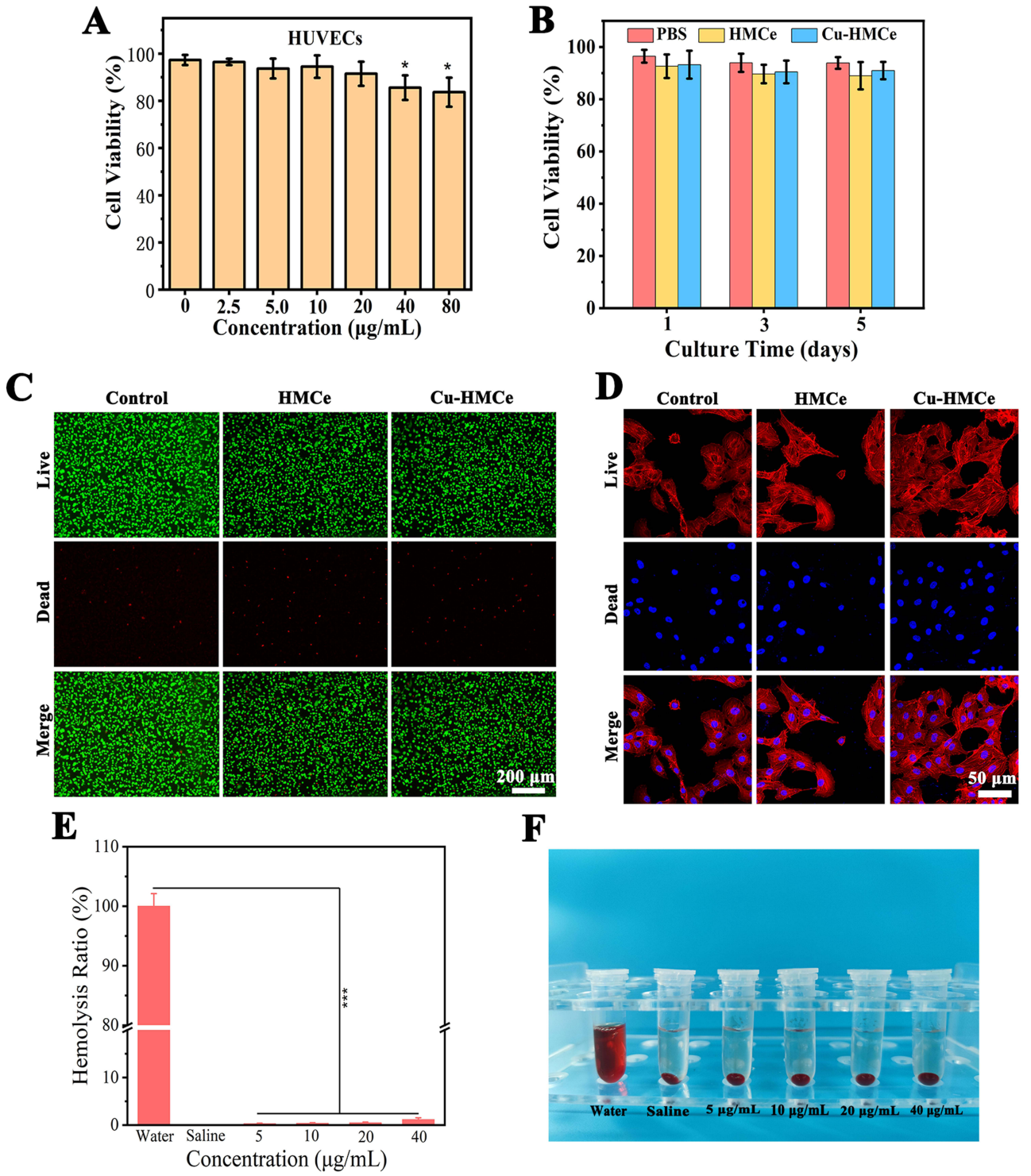

Figure 2 (**A**) Cell viability of HUVECs co-cultured with different concentrations of Cu-HMCe. (**B**) Cell viability of HUVECs co-cultured with control, HMCe, and Cu-HMCe for 1, 3, and 5 days. (**C**) Live/dead assays. (**D**) CLSM images of HUVECs morphology after 3 days of control, HMCe and Cu-HMCe treatment. (**E**) Hemolysis ratio and (**F**) Images of fresh mouse erythrocytes co-cultured with different concentrations of Cu-HMCe. Significance levels of *p< 0.05 and ***p<0.001 were applied.

Furthermore, fresh mouse erythrocytes were applied to perform a hemolysis test to assess the hemocompatibility of Cu-HMCe. The results showed that Cu-HMCe exhibited good blood compatibility, as no significant hemolysis was observed even at high concentration (40 μg/mL), and the hemolysis rates were all less than 5% (Figure 2E). Besides, as showed in Figure 2F, the color of the supernatant of the blood cells after Cu-HMCe treatment showed a yellowish color

consistent with PBS treatment. These results indicate that the nanozymes are well biocompatible and safe enough for further in vivo experiments. Hollow mesoporous cerium oxide nanoparticles act as copper carriers for slow and sustained release of Cu^{2+}, preventing toxicity from excessive localized concentrations of Cu^{2+}.

Angiogenesis Experiment

The dysfunction of the vasculature is a significant impediment to chronic wound contraction.[33,34] To explore the in vitro angiogenesis of nanozymes and the impact of HUVECs on tissue revascularisation, we conducted cell migration and endothelial tube formation tests using HUVECs. The results of the cell migration assay showed a significant increase in cell migration in the HMCe and Cu-HMCe groups compared to the control group (Figure 3A and C). Furthermore, the Cu-HMCe group exhibited notably higher cell mobility when compared to the HMCe group, indicating that the presence

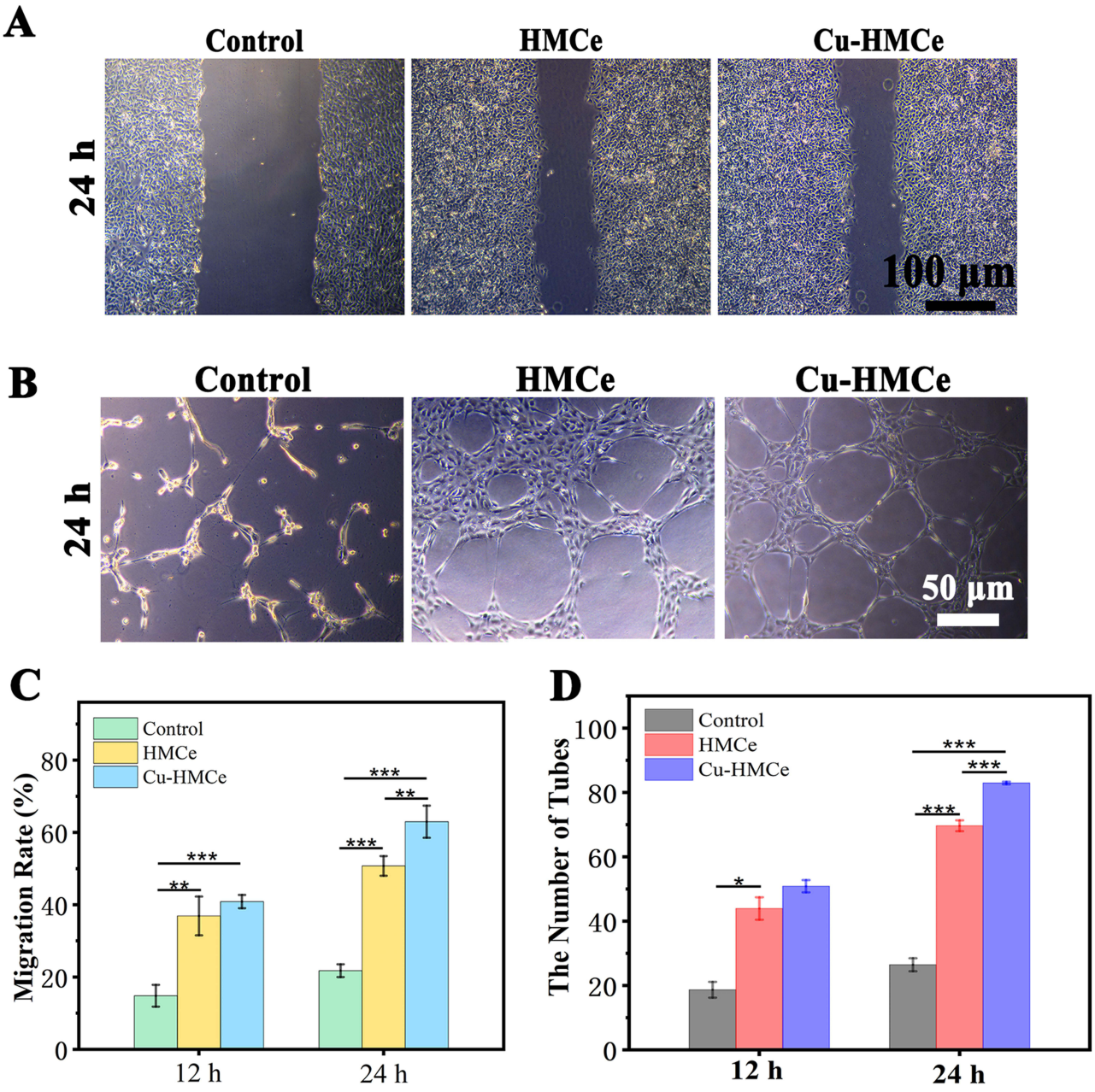

Figure 3 (**A**) migration assays and (**B**) tube formation assays of HUVECs co-cultured with control, HMCe and Cu-HMCe. Quantified analysis of (**C**) migration assays and (**D**) tube formation assays. Significance levels of *p< 0.05, **p< 0.01, and ***p<0.001 were applied.

of Cu had a positive impact on cellular migration, and this effect was further enhanced over time. After 24 h of co-culture, the cell migration rates were 21.8 ± 1.87%, 50.8 ± 2.7% and 63 ± 4.5% in the control, HMCe and Cu-HMCe groups, respectively. We further evaluated the effect of resulting nanozymes on the tubular formation of HUVECs. As shown in Figure 3B, after 24 h of co-culture, HUVECs in the control group formed fewer tubes, whereas an intact tubular network of HUVECs was observed in the Cu-HMCe group. Figure 3D further showed that the number of tubes is significantly higher in the HMCe and Cu-HMCe groups, with the Cu-HMCe group having the highest number of tubes compared to the control group. These findings suggested that Cu-HMCe exhibited a beneficial impact on the migration of cells and angiogenesis in vitro. This could potentially be attributed to the incorporation of Cu into HMCe. Cu is an important cofactor for many enzymes, some of which play key roles in angiogenesis. In previous studies, Cu has been shown to affect the proliferation and migration of vascular endothelial cells, contributing to angiogenesis and repair of damaged blood vessels.[3,31] Synergistic interaction of HMCe and Cu in Cu-HMCe enhances the microenvironment for the movement and formation of tubes by HUVECs.

Antibacterial Activities of Nanozymes

The maintenance of antibacterial activity to manage infections is imperative for wound recovery. In order to explore the in vitro antibacterial proficiency of the nanozymes, the turbidimetry method was employed. As depicted in Figure 4A and B, Cu-HMCe nanozymes exhibited strong antibacterial properties against both *S. aureus* and *E. coli* compared to PBS and HMCe. Additionally, the antimicrobial effectiveness of Cu-HMCe increased gradually over time, which may be related to the continuous release of the antibacterial Cu element. The excellent antimicrobial effect of nanozymes is mainly attributed to the antimicrobial properties of HMCe and Cu^{2+}. HMCe is able to affect bacterial viability by inducing oxidative stress and interfering with nutrient transport functions.[35] Cu^{2+} released by nanozymes can act on bacteria by destroying their cellular structure, inducing oxidative stress, interfering with enzyme activity, and interfering with intracellular metal ion balance, leading to bacterial inhibition and death.[36] In addition, the irregular shape and rough edges of Cu-HMCe can cause mechanical damage to the bacterial membrane.

The typical microenvironment of a chronically infected wound is usually characterized by an acidic matrix due to the production of multiple acidic metabolites by bacteria during infection.[37] The pH response capability of Cu-HMCe was evaluated by incubating it with different pH medium solutions. The results showed that Cu-HMCe exhibited a unique acid-responsive release pattern (Figure 4C). In a neutral medium, the cumulative Cu release was only about 20% over 80 hours. However, in an acidic solution, Cu release reached above 60% within 24 hours and continued consistently. It can be concluded that the release of Cu was promoted by acidic environment. This result suggests that Cu-HMCe has great potential for application in acidified chronic refractory wounds with bacterial infections. The responsive release of Cu^{2+} in acidified wounds could help to improve its utilization and efficacy.

In vitro Evaluation of Antioxidant Activity

Reactive oxygen species (ROS) include a variety of molecules such as superoxide anion (O_2^-), hydrogen peroxide (H_2O_2) and hydroxyl radical (-OH). Studies have shown that appropriate oxidative stress is beneficial for promoting tissue regeneration and repair, while excessive oxidative stress is detrimental to tissue repair.[38,39] Therefore, the ability to scavenge ROS is also a key indicator of wound healing promoting nanozymes. In the DPPH assays, the Cu-HMCe exhibited the highest free radical scavenging ability, which gradually increased over time (Figure 4D and E). Quantitative analysis revealed that the Cu-HMCe successfully eliminated over 80% of the free radicals (Figure 4F). To further explore the antioxidant properties of Cu-HMCe, hydroxyl radical (OH) was selected as a representative ROS to investigate the scavenging abilities of Cu-HMCe. As with the prior results, the colorimetric TMB assays revealed that Cu-HMCe displayed excellent OH scavenging ability compared to the other two groups (Figure 4G). ESR spectra also showed the low characteristic signal of OH for Cu-HMCe (Figure 4H). Furthermore, the results of the ROS staining indicated a notable decrease in DCFH-DA positive cells in the Cu-HMCe group, as compared to the control group (Figure 4I). These findings suggest that Cu-HMCe exhibits excellent antioxidant enzyme-mimetic activity, effectively scavenging reactive oxygen species and demonstrating good antioxidant properties. This is mainly due to the fact that cerium oxide nanoparticles can scavenge excess free radicals by continuously

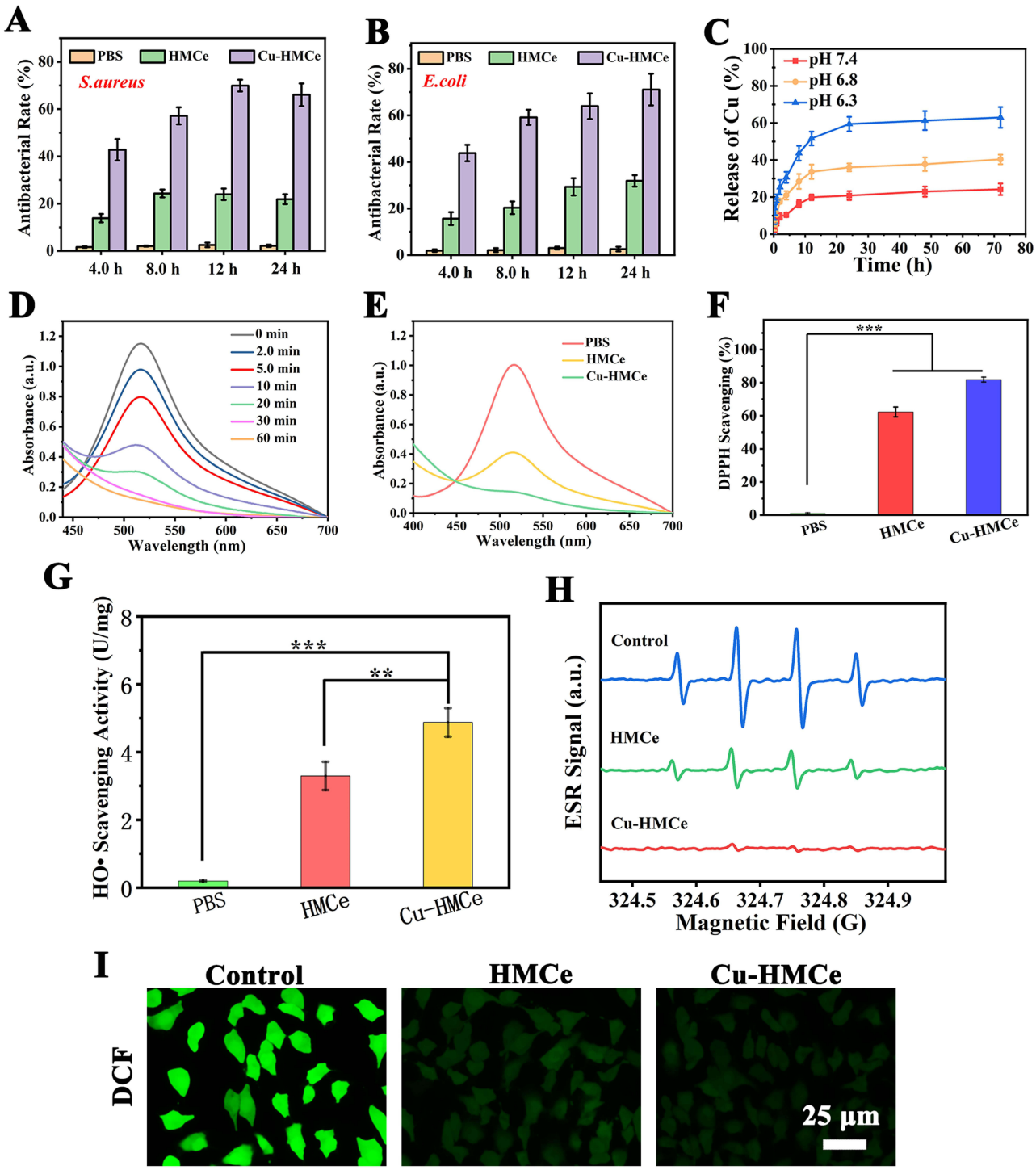

Figure 4 Antibacterial sensitivity of nanozymes. (**A**) The antibacterial rate of S. aureus and (**B**) E. coli. (**C**) pH-dependent release of Cu in Cu-HMCe. (**D**) Time-dependent scavenging of free radicals of Cu-HMCe. (**E**) Free radical eliminating activity of control, HMCe or Cu-HMCe. (**F**) Quantified analysis of DPPH assays. (**G**) and (**H**) OH scavenging ability of control, HMCe or Cu-HMCe. (**I**) ROS staining of control, HMCe or Cu-HMCe. Significance levels of, $^{**}p< 0.01$ and $^{***}p<0.001$ were applied.

participating in the process of reducing Ce (IV) and oxidizing Ce (III) in a redox cycle. Therefore, Cu-HMCe can reduce excessive oxidative stress at the wound site, protect cells and tissues from post oxidative damage, and provide a favorable microenvironment for wound repair.

In vivo Wound Healing Experiments

Next, a model of a full-thickness wound defect was created to evaluate the healing properties of Cu-HMCe nanozymes on skin injuries. In the Figure 5A, it can be seen that all groups showed a gradual decrease in wound size over time. Of note, the wound healing rate of Cu-HMCe and HMCe treatment groups was faster than that of other groups. Within two weeks of treatment, the Cu-HMCe group had almost fully healed wounds covered with new epithelium. At the same time, the control group and the Cu^{2+} group still had open wounds, while the HMCe group had small closed wounds with eschars. Consequently, these findings indicate that the inclusion of Cu into HMCe has boosted the capacity to facilitate wound healing.

To examine the process of healing and regeneration, H&E staining and Masson staining were conducted on wound specimens obtained from various treated groups. After 14 days of treatment, the control and Cu^{2+} groups exhibited congestion in the dermal layer, while the HMCe group showed persistent damage in the epithelialized tissue. On the contrary, the Cu-HMCe group exhibited the generation of intact dermal and epithelial formations within the recovered tissue (Figure 5D). As the epithelium acts as a protective barrier against pathogen infection, evaluating re-epithelialization is crucial for wound healing.[40] Quantitative analysis revealed that the Cu-HMCe treated group exhibited the highest rate of re-epithelialization (Figure 5B). Additionally, collagen deposition is a key biomarker for damaged skin healing.[41] Masson staining and quantitative analysis demonstrated that the Cu-HMCe treated group had significantly denser collagen deposition compared to the other three groups (Figure 5C). Consequently, these findings demonstrate that Cu-HMCe can substantially facilitate epidermal remodeling and accelerate wound healing.

In vivo Evaluation of the Anti-Inflammatory and Vascularization Properties of Nanozymes

To gain deeper insights into the mechanisms underlying the wound-healing effects of nanozymes, we performed immunohistochemical staining to evaluate the inflammatory response during skin injury. TNF-α, IL-6, and IL-1β represent prominent pro-inflammatory cytokines that serve as crucial markers of inflammation.[42,43] Immunohistochemical analysis showed that the

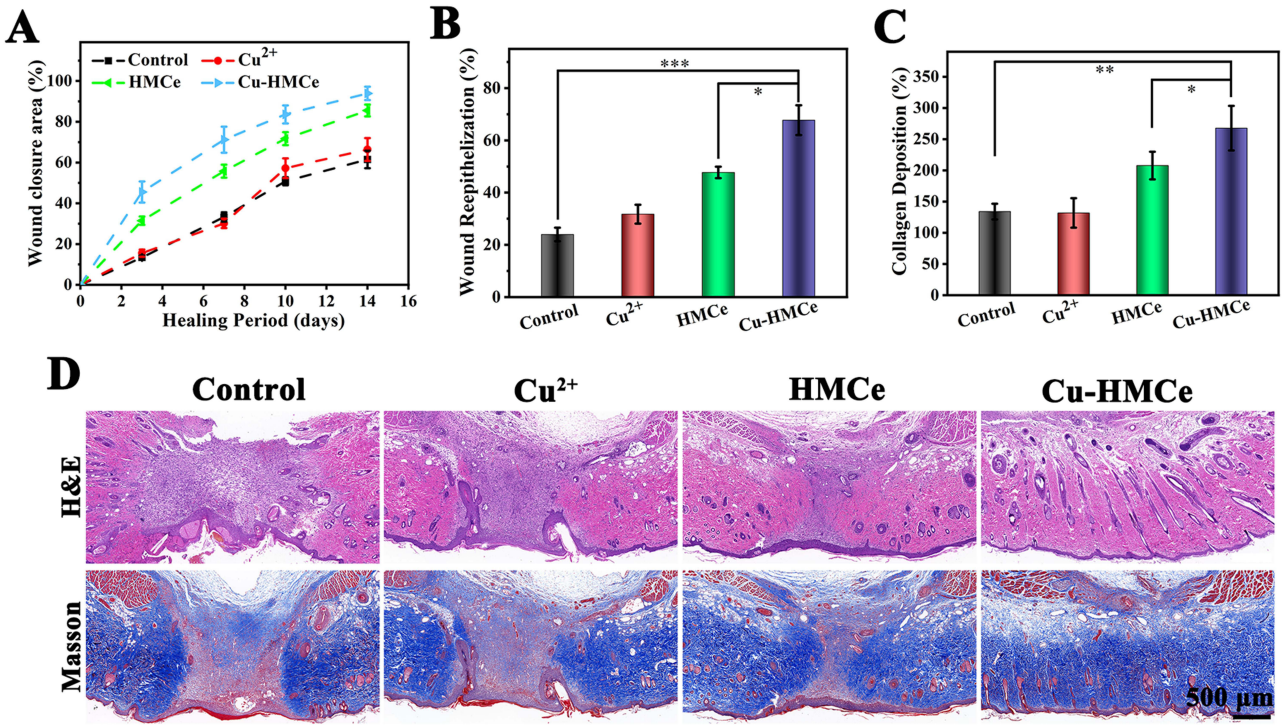

Figure 5 (**A**) The wound closure rates within 14 days after surgery. Corresponding quantitative analysis of the (**B**) wound re-epithelization and (**C**) collagen deposition on 14 days. (**D**) Histological analysis of wound tissues at 14 days. Significance levels of *p< 0.05, **p< 0.01, and ***p<0.001 were applied.

Cu-HMCe group displayed the lowest percentage of inflammatory cells expressing TNF-α and IL-6 at 10 days postoperatively, whereas the control group expressed the highest inflammatory factors (Figure 6A). Figures 6B and C also showed that the wound tissue's production of TNF-α or IL-6 was notably lower in the HMCe and Cu-HMCe groups compared to the other two groups. These findings indicate that Cu-HMCe is effective in preventing the inflammatory response in cutaneous wounds.

The ability of the nanoenzymes to promote neovascularization in vivo was further explored by CD31 immunohistochemical staining. In the early postoperative period, there was no significant difference in the formation of neovascularization between all groups. While at 10-day post-surgery, both the HMCe and Cu-HMCe treated groups exhibited

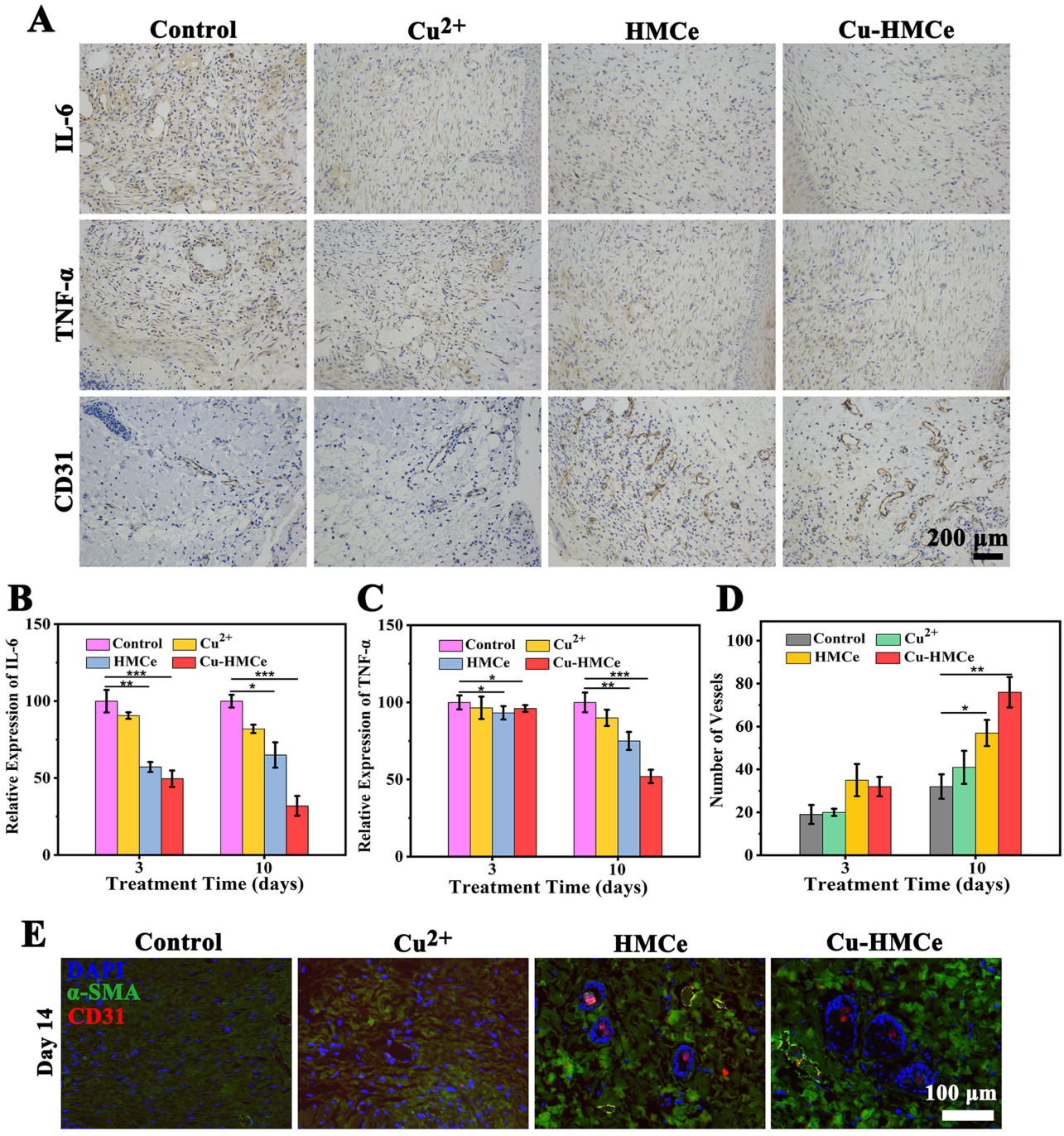

Figure 6 (**A**) Immunohistochemical staining images for TNF-α, IL-6 or CD31 of the wound sections after 10-day treatment. Quantified analysis of the relative expression of (**B**) IL-6 and (**C**) TNF-α. (**D**) Quantified analysis of the number of vessels. (**E**) Immunofluorescence staining images for CD31 and α-SMA of the wound sections after 14-day treatment. Significance levels of *$p< 0.05$, **$p< 0.01$, and ***$p<0.001$ were applied.

increased neovascularization formation. The Cu-HMCe group displayed the highest increase, which can be attributed to the angiogenic properties of the Cu component (Figure 6D). Meanwhile, Cu-HMCe demonstrated promising anti-inflammatory capabilities which facilitated the development of blood circulation, thereby considerably enhancing the formation of neovascularization.

The revascularization ability of Cu-HMCe is further confirmed by conducting CD31 (red) and α-SMA (green) immunofluorescence staining on HUVECs. As depicted in Figure 6E, Cu-HMCe displayed noticeably heightened CD31 and α-SMA expression, while HMCe exhibited a moderate level of expression. Conversely, the control and Cu^{2+} group showcased a lower level of CD31 and α-SMA expression. This conclusively demonstrated the potential of Cu-HMCe in accelerating wound regeneration by promoting vascularization through up-regulation of CD31 and α-SMA expression. Thus, it was fully proven that the Cu-HMCe had the ability to promote angiogenesis in vivo, which was better than the application of Cu^{2+} or HMCe alone.

Overall, the obtained nanozymes have demonstrated their ability to effectively suppress the inflammatory micro-environment and promote angiogenesis, which in turn accelerates the healing of wounds. This integration of functions showcases the synergistic effects of the nanozymes in facilitating wound repair.

Conclusions

In summary, we reported a copper-doped cerium oxide nanozymes with hollow mesopores, showing excellent porosity, stability, and biocompatibility. In vitro experiments highlighted the promotion of endothelial cell proliferation and migration. Further, in vivo and in vitro experiments supported multiple ways it promotes wound healing, such as antioxidation, improving the local inflammatory environment, and promoting neovascularization. According to the study, Cu-HMCe nanozymes with multi-functionality have the potential to significantly enhance wound healing. Such findings offer a glimpse into a promising future where multifunctional Cu-HMCe nanozymes hold the key to more efficient, cost-effective, and patient-centric solutions for skin wound management. However, in order to make Cu-HMCe closer to clinical application, it is necessary to further study its biosafety and promoting vascularization mechanism.

Acknowledgments

The authors gratefully acknowledge financial support from the Basic and Applied Basic Research Foundation of Guangdong Province (Grant Number: 2023A1515012615), the Enterprise Joint Fund for Basic and Applied Basic Research of Guangdong Province (Grant Number: 2022A1515220157), the Project of Administration of Traditional Chinese Medicine of Guangdong Province of China (Grant Number: 20231026), Guangzhou Natural Science Foundation (Grant Number: 202102021284), Natural Science Foundation of Guangdong Province (Grant Number: 2021A1515111158) and the National Natural Science Foundation of China (Grant Number: 32300962).

Disclosure

The authors report no conflicts of interest in this work.

References

1. Xu R, Fang Y, Zhang Z, et al. Recent advances in biodegradable and biocompatible synthetic polymers used in skin wound healing. *Materials*. 2023;16(15):5459. doi:10.3390/ma16155459
2. Sen CK. Human wound and its burden: updated 2022 compendium of estimates. *Adv Wound Care*. 2023;12(12):657–670. doi:10.1089/wound.2023.0150
3. Alizadeh S, Seyedalipour B, Shafieyan S, et al. Copper nanoparticles promote rapid wound healing in acute full thickness defect via acceleration of skin cell migration, proliferation, and neovascularization. *Biochem Biophys Res Commun*. 2019;517(4):684–690. doi:10.1016/j.bbrc.2019.07.110
4. Aulanni'am A, Ora KM, Ariandini NA, et al. Wound healing properties of Gliricidia sepium leaves from Indonesia and the Philippines in rats (Rattus norvegicus). *Vet World*. 2021;14(3):820–824. doi:10.14202/vetworld.2021.820-824
5. Wilkinson HN, Hardman MJ. Wound healing: cellular mechanisms and pathological outcomes. *Open Biol*. 2020;10(9):200223. doi:10.1098/rsob.200223
6. Ataide JA, Zanchetta B, Santos ÉM, et al. Nanotechnology-based dressings for wound management. *Pharmaceuticals*. 2022;15(10):1286. doi:10.3390/ph15101286
7. Cui L, Liang J, Liu H, et al. Nanomaterials for angiogenesis in skin tissue engineering. *Tissue Eng Part B Rev*. 2020;26(3):203–216. doi:10.1089/ten.teb.2019.0337

8. Nussbaum SR, Carter MJ, Fife CE, et al. An economic evaluation of the impact, cost, and medicare policy implications of chronic nonhealing wounds. *Value Health*. 2018;21(1):27–32. doi:10.1016/j.jval.2017.07.007
9. Komi DEA, Khomtchouk K, Santa Maria PL. Review of the Contribution of Mast Cells in Wound Healing: involved Molecular and Cellular Mechanisms. *Clin Rev Allergy Immunol*. 2020;58(3):298–312. doi:10.1007/s12016-019-08729-w
10. Vasalou V, Kotidis E, Tatsis D, et al. The Effects of Tissue Healing Factors in Wound Repair Involving Absorbable Meshes: a Narrative Review. *J Clin Med*. 2023;12(17):5683. doi:10.3390/jcm12175683
11. Gonzalez AC, Costa TF, Andrade ZA, et al. Wound healing - A literature review. *Anais brasileiros de dermatologia*. 2016;91(5):614–620. doi:10.1590/abd1806-4841.20164741
12. Manning-Geist BL, Cowan RA, Schlappe B, et al. Assessment of wound perfusion with near-infrared angiography: a prospective feasibility study. *Gynecol Oncol Rep*. 2022;40:100940. doi:10.1016/j.gore.2022.100940
13. Han G, Ceilley R. Chronic Wound Healing: a Review of Current Management and Treatments. *Adv Therapy*. 2017;34(3):599–610. doi:10.1007/s12325-017-0478-y
14. Powers JG, Higham C, Broussard K, et al. Wound healing and treating wounds: chronic wound care and management. *J Am Acad Dermatol*. 2016;74(4):607–625. doi:10.1016/j.jaad.2015.08.070
15. Huang SM, Wu CS, Chiu MH, et al. High glucose environment induces M1 macrophage polarization that impairs keratinocyte migration via TNF-α: an important mechanism to delay the diabetic wound healing. *J Dermatological Sci*. 2019;96(3):159–167. doi:10.1016/j.jdermsci.2019.11.004
16. Zhang Y, Wang S, Yang Y, et al. Scarless wound healing programmed by core-shell microneedles. *Nat Commun*. 2023;14(1):3431. doi:10.1038/s41467-023-39129-6
17. Kharaziha M, Baidya A, Annabi N. Baidya A Annabi N Rational Design of Immunomodulatory Hydrogels for Chronic Wound Healing. *Adv Mater*. 2021;33(39):e2100176. doi:10.1002/adma.202100176
18. Sies H, Jones DP. Reactive oxygen species (ROS) as pleiotropic physiological signalling agents. *Nat Rev Mol Cell Biol*. 2020;21(7):363–383. doi:10.1038/s41580-020-0230-3
19. Weng P, Liu K, Yuan M, et al. Development of a ZIF-91-Porous-Liquid-Based Composite Hydrogel Dressing System for Diabetic Wound Healing. *Small*. 2023;19(25):e2301012. doi:10.1002/smll.202301012
20. Sies H, Belousov VV, Chandel NS, et al. Defining roles of specific reactive oxygen species (ROS) in cell biology and physiology. *Nat Rev Mol Cell Biol*. 2022;23(7):499–515. doi:10.1038/s41580-022-00456-z
21. Ali F, Khan I, Chen J, et al. Emerging Fabrication Strategies of Hydrogels and Its Applications. *Gels*. 2022;8(4). doi:10.3390/gels8040205
22. Xiao Y, Xu M, Lv N, et al. Dual stimuli-responsive metal-organic framework-based nanosystem for synergistic photothermal/pharmacological antibacterial therapy. *Acta Biomater*. 2021;122:291–305. doi:10.1016/j.actbio.2020.12.045
23. Pan W, Wu B, Nie C, et al. NIR-II Responsive Nanohybrids Incorporating Thermosensitive Hydrogel as Sprayable Dressing for Multidrug-Resistant-Bacteria Infected Wound Management. *ACS nano*. 2023;17(12):11253–11267. doi:10.1021/acsnano.2c10742
24. Qi Y, Qian K, Chen J, et al. A thermoreversible antibacterial zeolite-based nanoparticles loaded hydrogel promotes diabetic wound healing via detrimental factor neutralization and ROS scavenging. *J Nanobiotechnol*. 2021;19(1):414. doi:10.1186/s12951-021-01151-5
25. Ryu TK, Lee H, Yon DK, et al. The antiaging effects of a product containing collagen and ascorbic acid: in vitro, ex vivo, and pre-post intervention clinical trial. *PLoS One*. 2022;17(12):e0277188. doi:10.1371/journal.pone.0277188
26. Wang X, Liu T, Chen M, et al. An Erythrocyte-Templated Iron Single-Atom Nanozyme for Wound Healing. *Adv Sci*. 2024;11(6):e2307844. doi:10.1002/advs.202307844
27. Huang W, Xu P, Fu X, et al. Functional molecule-mediated assembled copper nanozymes for diabetic wound healing. *J Nanobiotechnol*. 2023;21(1):294. doi:10.1186/s12951-023-02048-1
28. Nosrati H, Heydari M, Khodaei M. Cerium oxide nanoparticles: synthesis methods and applications in wound healing. *Mater Today Bio*. 2023;23:100823. doi:10.1016/j.mtbio.2023.100823
29. Lusvardi G, Sgarbi Stabellini F, Salvatori R. P(2)O(5)-Free Cerium Containing Glasses: bioactivity and Cytocompatibility Evaluation. *Materials*. 2019;12(19):3267.
30. Diao W, Li P, Jiang X, et al. Progress in copper-based materials for wound healing. *Wound Repair Regener*. 2023. doi:10.1111/wrr.13122
31. Salvo J, Sandoval C. Role of copper nanoparticles in wound healing for chronic wounds: literature review. *Burns Trauma*. 2022;10. doi:10.1093/burnst/tkab047
32. Xiao J, Zhu Y, Huddleston S, et al. Copper Metal-Organic Framework Nanoparticles Stabilized with Folic Acid Improve Wound Healing in Diabetes. *ACS nano*. 2018;12(2):1023–1032. doi:10.1021/acsnano.7b01850
33. Kim N, Lee H, Han G, et al. 3D-Printed Functional Hydrogel by DNA-Induced Biomineralization for Accelerated Diabetic Wound Healing. *Adv Sci*. 2023;10(17):e2300816. doi:10.1002/advs.202300816
34. Hu Y, Xiong Y, Tao R, et al. Advances and perspective on animal models and hydrogel biomaterials for diabetic wound healing. *Biomater Transl*. 2022;3(3):188–200. doi:10.12336/biomatertransl.2022.03.003
35. Zhang M, Zhang C, Zhai X, et al. Antibacterial mechanism and activity of cerium oxide nanoparticles. *Sci China Mater*. 2019;62(11):1727–1739. doi:10.1007/s40843-019-9471-7
36. Grass G, Rensing C, Solioz M. Rensing C Solioz M Metallic copper as an antimicrobial surface. *Appl Environ Microbiol*. 2011;77(5):1541–1547. doi:10.1128/AEM.02766-10
37. Wang X, Shan M, Zhang S, et al. Stimuli-Responsive Antibacterial Materials: molecular Structures, Design Principles, and Biomedical Applications. *Adv Sci*. 2022;9(13):e2104843. doi:10.1002/advs.202104843
38. Serras F. Serras F The benefits of oxidative stress for tissue repair and regeneration. *Fly*. 2016;10(3):128–133. doi:10.1080/19336934.2016.1188232
39. Yang G, Chen H, Chen Q, et al. Injury-induced interleukin-1 alpha promotes Lgr5 hair follicle stem cells de novo regeneration and proliferation via regulating regenerative microenvironment in mice. *Inflam Regenerat*. 2023;43(1):14. doi:10.1186/s41232-023-00265-7
40. Yu M, Huang J, Zhu T, et al. Liraglutide-loaded PLGA/gelatin electrospun nanofibrous mats promote angiogenesis to accelerate diabetic wound healing via the modulation of miR-29b-3p. *Biomater Sci*. 2020;8(15):4225–4238. doi:10.1039/D0BM00442A
41. Dong Y, Zhuang H, Hao Y, et al. Poly(N-Isopropyl-Acrylamide)/Poly(γ-Glutamic Acid) Thermo-Sensitive Hydrogels Loaded with Superoxide Dismutase for Wound Dressing Application. *Int j Nanomed*. 2020;15:1939–1950. doi:10.2147/IJN.S235609

42. Sheng F, Zhang L, Wang S, et al. Deacetyl Ganoderic Acid F Inhibits LPS-Induced Neural Inflammation via NF-κB Pathway Both In Vitro and In Vivo. *Nutrients*. 2019;12(1):85. doi:10.3390/nu12010085
43. Sun Y, Chen X, Shi S, et al. Tetrahedral Framework Nucleic Acids: a Novel Strategy for Antibiotic Treating Drug-Resistant Infections. *Biomacromolecules*. 2023;24(2):1052–1060. doi:10.1021/acs.biomac.2c01525

International Journal of Nanomedicine Dovepress

Publish your work in this journal

The International Journal of Nanomedicine is an international, peer-reviewed journal focusing on the application of nanotechnology in diagnostics, therapeutics, and drug delivery systems throughout the biomedical field. This journal is indexed on PubMed Central, MedLine, CAS, SciSearch®, Current Contents®/Clinical Medicine, Journal Citation Reports/Science Edition, EMBase, Scopus and the Elsevier Bibliographic databases. The manuscript management system is completely online and includes a very quick and fair peer-review system, which is all easy to use. Visit http://www.dovepress.com/testimonials.php to read real quotes from published authors.

Submit your manuscript here: https://www.dovepress.com/international-journal-of-nanomedicine-journal